Analytical Estimation of Radar Cross Section of Infinitely Long Conducting Cylinder Coated with Metamaterial

Girish K.[1] and Hema Singh[2]

Abstract: Aerospace structures can be approximately modeled as a combination of canonical structures such as cylinder, cone and ellipsoid. Thus the RCS estimation of such canonical structures is of prime interest. Furthermore metamaterials possess peculiar electromagnetic properties which can be useful in modifying the RCS of structures. This paper is aimed at calculating the RCS of an infinitely long PEC circular cylinder coated with one or two layers of metamaterial. The incident and scattered fields of coated cylinder are expressed in terms of series summation of Bessel and Hankel functions. The unknown coefficients of summation are obtained by applying appropriate boundary conditions. The computations are carried out for both principal polarizations. The computed results are validated against the numerical-based method of moments. Further, the variation of RCS of the metamaterial coated PEC cylinder with material parameters, frequency, aspect angle and polarization is analyzed.

Keywords: Coated Cylinder, metamaterial, perfect electric conductor, radar cross section, polarization.

1 Introduction

The estimation of RCS of a complex structured target involves steps such as approximating the given structure in terms of canonical shapes, calculating RCS contribution from each of the individual canonical shapes and then appropriately summing individual contributions to arrive at overall RCS of the structure [Crispin and Siegel (1968)]. Thus, the RCS estimation of canonical structures is an important study towards scattering analysis of complex structures. RCS is a function of target geometry, constituent material parameters such as dielectric permittivity and permeability and incident wave properties such as frequency, angle of incidence and polarization. By an appropriate choice of material, RCS of the target can be controlled to some extent.

The RCS of a target is traditionally controlled by coating one or more layers of lossy dielectric material over the structure. However, since about a decade, extensive research is being carried out, to employ the peculiar electromagnetic (EM) characteristics of metamaterials for RCS control. Metamaterials can be classified as µ-negative (MNG, where

---

[1] RV College of Engineering, Bangalore, India

[2] CSIR-NAL, Bangalore, India

only permeability is negative), ε-negative (ENG, where only permittivity is negative) and double negative (DNG) materials [Capolino (2009)]. The materials with negative permittivity and permeability in the microwave frequency region were first practically realized in the year 2000 [Smith et al. (2000)]. In recent years, metamaterial has been used as radar absorbing materials (RAMs) [Chaurasiya and Ghosh (2014)] and frequency selective surfaces (FSS) [Shi et al. (2010)], for achieving low reflectivity over certain frequency bands. A detailed theoretical analysis of electromagnetic behavior of metamaterials may be obtained in Capolino [Capolino (2009)], where the FDTD computations of EM wave propagation in a DNG slab is discussed.

Various methods have been proposed for the estimation of RCS and can be categorized as numerical methods, high-frequency ray-theoretic methods, and hybrid methods [Jenn (2005); Eugene (1985)]. The finite-difference time-domain (FDTD) method involves the numerical implementation of differential form of Maxwell's equations. It is ideal for time domain visualization of the EM fields and frequency domain results can be extracted by applying fast Fourier transform (FFT) to the time-domain scattering parameters. However it has drawback of high computational complexity. On the other hand, the method of moments (MoM) is a numerical implementation of integral form of Maxwell's equations and it offers an accurate solution, but again has high computational cost. In high frequency methods, the simplest is geometric optics (GO) method, a ray-based method which assumes that specular points on the target contribute dominantly to the overall RCS. The methods based on physical optics (PO) and physical theory of diffraction (PTD), are limited to scattering from edges and corners. Other high-frequency methods such as uniform theory of diffraction (UTD) and uniform asymptotic theory (UAT) provide solution for scattered field in transition region, in the vicinity of the shadow region. These ray-theoretic methods mainly deal with conducting surfaces.

The scattering from coated conducting surfaces or non-conducting surfaces need the transmission to be taken into account apart from reflection and diffraction. This problem holds even for metamaterial-coated structures [Soares (2009); Kwon et al. (2009)]. The scattering from an infinitely long circular PEC cylinder coated with metamaterial has been analytically analyzed and compared with a similar cylinder coated with normal dielectric material [Li and Shen (2003); Irci and Erturk (2007)]. The cylindrical wave expanding theory has been applied for calculating far-field RCS of a PEC cylinder with two layer dielectric coating [Wu et al. (2015)]. The finite-difference frequency-domain (FDFD) method can also be used to estimate RCS of metamaterial-coated conducting cylinder and sphere [Zainuddeen and Botros (2008)]. In FDFD method, the frequency-domain form of Maxwell equations is iteratively solved to calculate the transmitted and the scattered fields. The scattering properties of a multilayered metamaterial cylinder have been analyzed by Yao et al. (2006) for both the principal polarizations, using the eigen-function expansion method. By enforcing the boundary conditions, the eigen coefficients are calculated iteratively to arrive at RCS.

In this paper, the RCS of an infinitely long perfect electrically conducting (PEC) circular cylinder coated with DNG metamaterials is determined. A closed form solution of EM wave scattering by metamaterial-coated circular cylinder of infinite length is analytically derived. The incident and scattered field are expanded in terms of Bessel and Hankel

functions. The appropriate boundary conditions are imposed to obtain the unknown coefficients for single-layer and double-layered lossless and homogeneous metamaterial coatings. The computed results are validated against MoM results available in open domain. The effect of frequency, constitutive parameters of metamaterial coating, and polarization has been analyzed. The parametric analysis of metamaterial-coated cylinder is geared towards RCS reduction over set of frequencies.

2 Analytical formulation of RCS of metamaterial coated cylinder

Single Layer Coating: A PEC circular cylinder of radius a coated with single layer of DNG type metamaterial is shown in Figure 1. The coating thickness is t_1 and the material parameters are $(-\mu_1, -\varepsilon_1)$. A uniform plane EM wave is incident at an angle φ_o, to the cylinder.

For TM_z polarization, incident field components are expressed as [Balanis (2012)],

$$E_z^i = \sum_{n=-\infty}^{\infty} j^{-n} J_n(\beta_o r) \; exp\,(jn(\varphi - \varphi_o)) \tag{1}$$

$$H_\varphi^i = \frac{-j}{\eta_o} \sum_{n=-\infty}^{\infty} j^{-n} J_n^{'}(\beta_o r) \; exp\,(jn(\varphi - \varphi_o)) \tag{2}$$

For TE_z polarization, the incident field components are given by

$$E_\varphi^i = \sum_{n=-\infty}^{\infty} j^{-n} J_n^{'}(\beta_o r) \; exp\,(jn(\varphi - \varphi_o)) \tag{3}$$

$$H_z^i = \frac{-j}{\eta_o} \sum_{n=-\infty}^{\infty} j^{-n} J_n(\beta_o r) \; exp\,(jn(\varphi - \varphi_o)) \tag{4}$$

where $\beta_o = \omega\sqrt{\mu_o \varepsilon_o}$; $\eta_o = \sqrt{\mu_o / \varepsilon_o}$; $J_n(x)$ is the Bessel function of first kind and n^{th} order; $J_n^{'}(x) = \frac{\partial}{\partial x} J_n(x)$
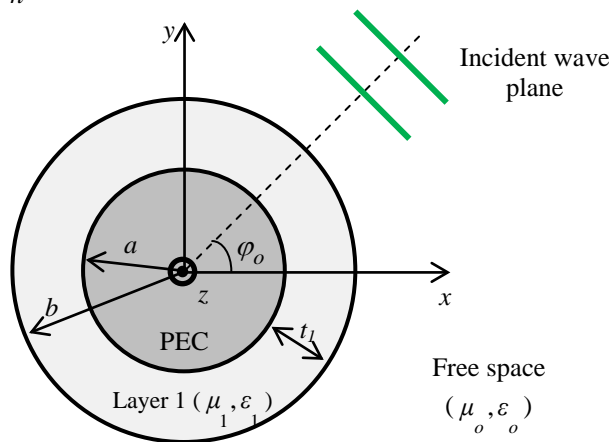

Figure 1: PEC cylinder with single layer coating

The scattered fields are travelling waves and can be represented in terms of the infinite summation of cylindrical Hankel functions. Thus, irrespective of polarization of incident waves, the scattered field components are expressed as,

$$E_z^S = \sum_{n=-\infty}^{\infty} j^{-n} A_n^m H_n^{(1)}(\beta_o r) \ exp(jn(\varphi - \varphi_o)) \tag{5}$$

$$H_\varphi^S = \frac{-j}{\eta_o} \sum_{n=-\infty}^{\infty} j^{-n} A_n^m H_n^{'(1)}(\beta_o r) \ exp(jn(\varphi - \varphi_o)) \tag{6}$$

$$E_\varphi^S = \sum_{n=-\infty}^{\infty} j^{-n} A_n^e H_n^{'(1)}(\beta_o r) \ exp(jn(\varphi - \varphi_o)) \tag{7}$$

$$H_z^S = \frac{-j}{\eta_o} \sum_{n=-\infty}^{\infty} j^{-n} A_n^e H_n^{(1)}(\beta_o r) \ exp(jn(\varphi - \varphi_o)) \tag{8}$$

Here, A_n^e and A_n^m are unknown coefficients for TE_z and TM_z polarizations. $H_n^{(1)}(x)$ is the Hankel function of first kind and n^{th} order; and $H_n^{'(1)}(x) = \frac{\partial}{\partial x} H_n^{(1)}(x)$

The fields inside Layer 1 are standing waves represented by infinite summation of Bessel wave functions [Yao (2006)]. For TM_z polarization, the field components inside Layer 1 are

$$E_z^1 = \sum_{n=-\infty}^{\infty} j^{-n} \ [a_n^{1m} J_n(\beta_1 r) + b_n^{1m} Y_n(\beta_1 r)] \ exp(jn(\varphi - \varphi_O)) \tag{9}$$

$$H_\varphi^1 = \frac{-j}{\eta_1} \sum_{n=-\infty}^{\infty} j^{-n} \ [a_n^{1m} J_n^{'}(\beta_1 r) + b_n^{1m} Y_n^{'}(\beta_1 r)] \ exp(jn(\varphi - \varphi_O)) \tag{10}$$

For TE_z polarization, the field components are

$$H_z^1 = \frac{-j}{\eta_1} \sum_{n=-\infty}^{\infty} j^{-n} \ [a_n^{1e} J_n(\beta_1 r) + b_n^{1e} Y_n(\beta_1 r)] \ exp(jn(\varphi - \varphi_O)) \tag{11}$$

$$E_\varphi^1 = \sum_{n=-\infty}^{\infty} j^{-n} \ [a_n^{1e} J_n^{'}(\beta_1 r) + b_n^{1e} Y_n^{'}(\beta_1 r)] \ exp(jn(\varphi - \varphi_O)) \tag{12}$$

Double Layer Coating: A PEC circular cylinder of radius *a,* with two layers of coating is shown in Figure 2. The thickness of Layer 1 and Layer 2 are t_1 and t_2 respectively. The fields inside Layer 1 are same as in (9)-(12). The field components inside Layer 2 are given by,

$$E_z^2 = \sum_{n=-\infty}^{\infty} j^{-n} \, [a_n^{2m} J_n(\beta_2 r)$$
$$+ \, b_n^{2m} Y_n(\beta_2 r)] \; exp(jn(\varphi - \varphi_o)) \tag{13}$$

$$H_\varphi^2 = \frac{-j}{\eta_1} \sum_{n=-\infty}^{\infty} j^{-n} \, [a_n^{2m} J_n'(\beta_2 r)$$
$$+ \, b_n^{2m} Y_n'(\beta_2 r)] \; exp(jn(\varphi - \varphi_o)) \tag{14}$$

$$H_z^2 = \frac{-j}{\eta_1} \sum_{n=-\infty}^{\infty} j^{-n} \, [a_n^{2e} J_n(\beta_2 r)$$
$$+ \, b_n^{2e} Y_n(\beta_2 r)] \; exp(jn(\varphi - \varphi_o)) \tag{15}$$

$$E_\varphi^2 = \sum_{n=-\infty}^{\infty} j^{-n} \, [a_n^{2e} J_n'(\beta_2 r)$$
$$+ \, b_n^{2e} Y_n'(\beta_2 r)] \; exp(jn(\varphi - \varphi_o)) \tag{16}$$
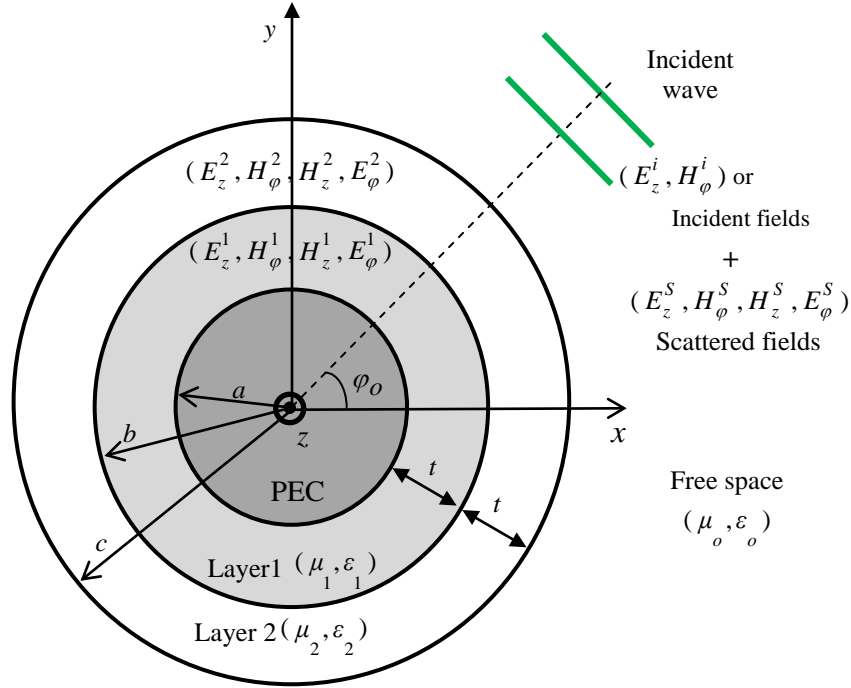

Figure 2: Structure of a PEC cylinder with two layers of coating

Here, a_n^{1m}, a_n^{1e}, b_n^{1m}, b_n^{1e} a_n^{2m}, a_n^{2e}, b_n^{2m} and b_n^{2e} are the unknown coefficients of summation to be determined using appropriate boundary conditions.

In order to obtain the scattering coefficients for single layer coated PEC circularcylinder, the following boundary conditions are imposed.

$$E^1_z\Big|_{r=a} = 0 \tag{17}$$

$$E^1_\varphi\Big|_{r=a} = 0 \tag{18}$$

$$E^1_z\Big|_{r=b} = E^i_z\Big|_{r=b} + E^s_z\Big|_{r=b} \tag{19}$$

$$H^1_z\Big|_{r=b} = H^i_z\Big|_{r=b} + H^s_z\Big|_{r=b} \tag{20}$$

$$E^1_\varphi\Big|_{r=b} = E^i_\varphi\Big|_{r=b} + E^s_\varphi\Big|_{r=b} \tag{21}$$

$$H^1_\varphi\Big|_{r=b} = H^i_\varphi\Big|_{r=b} + H^s_\varphi\Big|_{r=b} \tag{22}$$

On solving (17)-(22), one arrives at

$$A^m_n = \frac{a_1 c_2 - a_2 c_1}{a_2 b_1 - a_1 b_2} \tag{23}$$

$$A^e_n = \frac{a_3 c_4 - a_4 c_3}{a_4 b_3 - a_3 b_4} \tag{24}$$

where $a_1 = 1$; $a_3 = 1$; $b_1 = j^{-n} H^{(1)}_n(\beta_o b)\ exp(\text{-}jn\ \varphi_o)$

$$c_1 = j^{-n} J_n(\beta_o b)\ exp(\text{-}jn\ \varphi_o)$$

$$b_2 = \frac{1}{\eta_o} j^{-n} H'^{(1)}_n(\beta_o b)\ exp(\text{-}jn\ \varphi_o)$$

$$c_2 = \frac{1}{\eta_o} j^{-n} J'_n(\beta_o b)\ exp(\text{-}jn\ \varphi_o)$$

$$b_3 = j^{-n} H'^{(1)}_n(\beta_o b)\ exp(\text{-}jn\ \varphi_o)$$

$$c_3 = j^{-n} J'_n(\beta_o b)\ exp(\text{-}jn\ \varphi_o)$$

$$b_4 = \frac{1}{\eta_o} j^{-n} H^{(1)}_n(\beta_o b)\ exp(\text{-}jn\ \varphi_o)$$

$$c_4 = \frac{1}{\eta_o} j^{-n} J_n(\beta_o b)\ exp(\text{-}jn\ \varphi_o)$$

$$a_2 = \frac{1}{\eta_1}\left[\frac{J_n'(\beta_1 b)Y_n(\beta_1 a) - J_n(\beta_1 a)Y_n'(\beta_1 b)}{J_n(\beta_1 b)Y_n(\beta_1 a) - J_n(\beta_1 a)Y_n(\beta_1 b)}\right]$$

$$a_4 = \frac{1}{\eta_1}\left[\frac{J_n(\beta_1 b)\,Y_n'(\beta_1 a) - J_n'(\beta_1 a)Y_n(\beta_1 b)}{J_n'(\beta_1 b)\,Y_n'(\beta_1 a) - J_n'(\beta_1 a)\,Y_n'(\beta_1 b)}\right]$$

To obtain the scattering coefficients for two layer coating, the following boundary conditions are applied.

$$E_z^1\big|_{r=b} = E_z^2\big|_{r=b} \tag{25}$$

$$E_\varphi^1\big|_{r=b} = E_\varphi^2\big|_{r=b} \tag{26}$$

$$H_z^1\big|_{r=b} = H_z^2\big|_{r=b} \tag{27}$$

$$H_\varphi^1\big|_{r=b} = H_\varphi^2\big|_{r=b} \tag{28}$$

$$E_z^2\big|_{r=c} = E_z^i\big|_{r=c} + E_z^S\big|_{r=c} \tag{29}$$

$$H_z^2\big|_{r=c} = H_z^i\big|_{r=c} + H_z^S\big|_{r=c} \tag{30}$$

$$E_\varphi^2\big|_{r=c} = E_\varphi^i\big|_{r=c} + E_\varphi^S\big|_{r=c} \tag{31}$$

$$H_\varphi^2\big|_{r=c} = H_\varphi^i\big|_{r=c} + H_\varphi^S\big|_{r=c} \tag{32}$$

On solving (25)-(32), one obtains the scattering coefficients as follows:

$$A_n^m = \frac{d_m - e_1}{f_1} \tag{33}$$

$$A_n^e = \frac{d_e - e_2}{f_2} \tag{34}$$

where $d_m = d_1/d_2$; $d_e = d_3/d_4$; $d_1 = e_3 f_1 - e_1 f_3$

$d_3 = e_4 f_2 - e_2 f_4$; $d_4 = \dfrac{g_1 c_1 f_1}{a_1 - b_1} + h_1 f_1 - f_3$

$$d_4 = \frac{g_2 c_2 f_2}{a_2 - b_2} + h_2 f_2 - f_4$$

$$a_1 = \frac{1}{\eta_1}\left[\frac{J_n'(\beta_1 b)Y_n(\beta_1 a) - J_n(\beta_1 a)Y_n'(\beta_1 b)}{J_n(\beta_1 b)Y_n(\beta_1 a) - J_n(\beta_1 a)Y_n(\beta_1 b)}\right]$$

$$b_1 = \frac{1}{\eta_2}\left[\frac{J_n'(\beta_2 b)Y_n(\beta_2 c) - J_n(\beta_2 c)Y_n'(\beta_2 b)}{J_n(\beta_2 b)Y_n(\beta_2 c) - J_n(\beta_2 c)Y_n(\beta_2 b)}\right]$$

$$c_1 = \frac{1}{\eta_2}\left[\frac{J_n(\beta_2 b)Y_n'(\beta_2 b) - J_n'(\beta_2 b)Y_n(\beta_2 b)}{J_n(\beta_2 b)Y_n(\beta_2 c) - J_n(\beta_2 c)Y_n(\beta_2 b)}\right]$$

$$a_2 = \frac{1}{\eta_1}\left[\frac{J_n(\beta_1 b)Y_n'(\beta_1 a) - J_n'(\beta_1 a)Y_n(\beta_1 b)}{J_n'(\beta_1 b)Y_n'(\beta_1 a) - J_n'(\beta_1 a)Y_n'(\beta_1 b)}\right]$$

$$b_2 = \frac{1}{\eta_2}\left[\frac{J_n(\beta_2 b)Y_n'(\beta_2 c) - J_n'(\beta_2 c)Y_n(\beta_2 b)}{J_n'(\beta_2 b)Y_n'(\beta_2 c) - J_n'(\beta_2 c)Y_n'(\beta_2 b)}\right]$$

$$c_2 = \frac{1}{\eta_2}\left[\frac{J_n'(\beta_2 b)Y_n(\beta_2 b) - J_n(\beta_2 b)Y_n'(\beta_2 b)}{J_n'(\beta_2 b)Y_n'(\beta_2 c) - J_n'(\beta_2 c)Y_n'(\beta_2 b)}\right]$$

$$e_1 = j^{-n}J_n(\beta_o c)\,exp\,(-jn\varphi_o) \qquad ; \qquad e_2 = j^{-n}J_n'(\beta_o c)\,exp\,(-jn\varphi_o)$$

$$e_3 = \frac{1}{\eta_o}j^{-n}J_n'(\beta_o c)\,exp\,(-jn\varphi_o) \qquad ; \qquad e_4 = \frac{1}{\eta_o}j^{-n}J_n(\beta_o c)\,exp\,(-jn\varphi_o)$$

$$f_1 = j^{-n}H_n^{(1)}(\beta_o c)\,exp\,(-jn\varphi_o) \qquad ; \qquad f_2 = j^{-n}H_n^{'(1)}(\beta_o c)\,exp\,(-jn\varphi_o)$$

$$f_3 = \frac{1}{\eta_o}j^{-n}H_n^{'(1)}(\beta_o c)\,exp\,(-jn\varphi_o)$$

$$f_4 = \frac{1}{\eta_o}j^{-n}H_n^{(1)}(\beta_o c)\,exp\,(-jn\varphi_o) \qquad g_1 = \frac{1}{\eta_2}\left[\frac{J_n'(\beta_2 c)Y_n(\beta_2 c) - J_n(\beta_2 c)Y_n'(\beta_2 c)}{J_n(\beta_2 b)Y_n(\beta_2 c) - J_n(\beta_2 c)Y_n(\beta_2 b)}\right]$$

$$g_2 = \frac{1}{\eta_2}\left[\frac{J_n(\beta_2 c)Y_n'(\beta_2 c) - J_n'(\beta_2 c)Y_n(\beta_2 c)}{J_n'(\beta_2 b)Y_n'(\beta_2 c) - J_n'(\beta_2 c)Y_n'(\beta_2 b)}\right]$$

$$h_1 = \frac{1}{\eta_2}\left[\frac{J_n(\beta_2 b)Y_n'(\beta_2 c) - J_n'(\beta_2 c)Y_n(\beta_2 b)}{J_n(\beta_2 b)Y_n(\beta_2 c) - J_n(\beta_2 c)Y_n(\beta_2 b)}\right]$$

$$h_2 = \frac{1}{\eta_2}\left[\frac{J_n'(\beta_2 b)\,Y_n(\beta_2 c) - J_n(\beta_2 c)Y_n'(\beta_2 c)}{J_n'(\beta_2 b)Y_n'(\beta_2 c) - J_n'(\beta_2 c)Y_n'(\beta_2 b)}\right]$$

The far scattered field approximation is used to determine the normalized bistatic cylinder RCS, given by [Li and Shen (2003)]

$$\frac{\sigma^{TM}}{\lambda_O} = \frac{2}{\pi}\left|\sum_{n=-\infty}^{\infty} A_n^m\, exp(jn(\varphi - \varphi_o))\right|^2 \tag{35}$$

$$\frac{\sigma^{TE}}{\lambda_O} = \frac{2}{\pi}\left|\sum_{n=-\infty}^{\infty} A_n^e\, exp(jn(\varphi - \varphi_o))\right|^2 \tag{36}$$

3 Results and discussion

The RCS of coated cylinder is computed using the above analytical expressions. The computed results are validated against MoM results available in open domain. Further, parametric analyses of RCS of metamaterial coated cylinder are carried out towards achieving RCS reduction over certain frequency range.
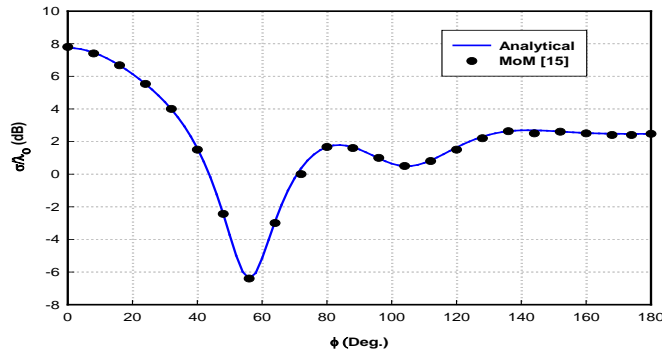

Figure 3: Variation of RCS of one layer metamaterial coated PEC circular cylinder of radius a=30 mm; coating thickness t_1= 6 mm (b= 36 mm), coating material is DNG, ε_{r1}= -4, μ_{r1}= -2; TM$_z$ polarization

A PEC circular cylinder with radius a=30 mm, coated with DNG type metamaterial is considered. The constitutive parameters of coating are t_1=6 mm, ε_{r1}= -4 and μ_{r1}= -2. The frequency is 5 GHz and polarization of incidence is TM$_z$. The RCS of the coated cylinder as a function of aspect angle is computed (Figure 3) and compared with the MoM results available in open domain [Sakr et al. (2014)]. It is apparent that there is an excellent match between the results of proposed analytical method and MoM.

Next, the RCS of single layer coated cylinder is compared with that of bare cylinder for the TM$_z$ mode (Figure 4). It is observed that the RCS of bare cylinder varies linearly with frequency in TM$_z$ polarization. The metamaterial coating results in reduction of RCS value over frequency range of 5.6-7.0 GHz.
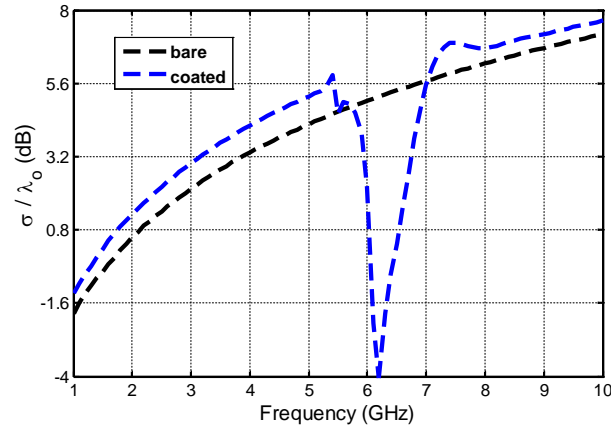
Figure 4: Variation of RCS of one layer metamaterial coated PEC circular cylinder of radius a=50 mm; coating thickness t_1=5 mm (b=55 mm), coating material is DNG, ε_{r1}=-4.65, μ_{r1}=-1; TM$_z$ polarization

Further, the RCS of a PEC circular cylinder with two layer coating is determined. The first layer coating is DNG metamaterial whereas second layer is a dielectric. The material parameters of coatings are $\varepsilon_{r1=}$-4, $\mu_{r1=}$-2, $\varepsilon_{r2=}$4 and $\mu_{r2=}$2. The thickness of metamaterial coating is t_1=6 mm (b=66 mm). The second layer thickness is t_2=6 mm (c=72 mm). The frequency is taken as 5 GHz. The RCS as a function of aspect angle is computed (Figure 5) and compared with MoM results available in open domain [Sakr et al. (2014)] for TM$_z$ polarization.

Next the thickness of coatings is increased. A PEC circular cylinder (a=60 mm) is considered with a metamaterial of thickness $t_{1=}$30 mm (b=90 mm) as first coating and a normal dielectric of thickness $t_{1=}$30 mm (c=120 mm) as second coating (DNG-DPS). The material characteristics of first coating are same as previous case i.e. ε_{r1}=- 4 and $\mu_{r1=}$-2, $\varepsilon_{r2=}$4 and μ_{r2}=2. The variation of cylinder RCS with aspect angle is computed (Figure 6) for TM$_z$ polarization. It may be observed that the RCS values computed analytically are in good agreement with those computed using MoM based integral equation solutions [Sakr et al. (2014)].
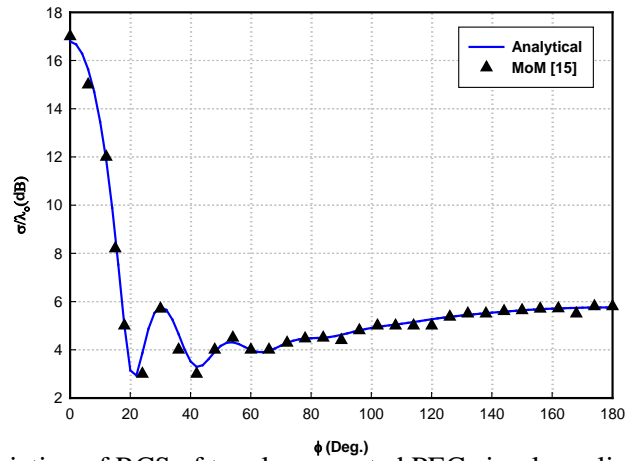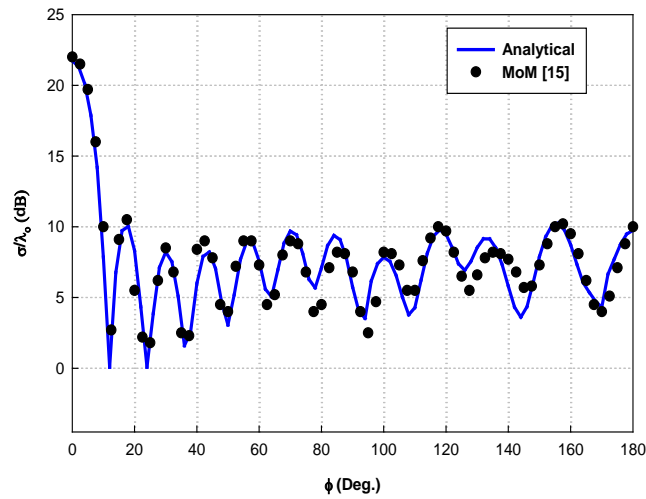
Figure 5: Variation of RCS of two layer coated PEC circular cylinder of radius *a*=60 mm; thickness of coatings is $t_1=t_2$=6 mm. DPS-DNG coating, $\varepsilon_{r1=}$-4, $\mu_{r1=}$-2, $\varepsilon_{r2=}$4, $\mu_{r2=}$2; *f*=5 GHz; TM$_z$ polarization

Figure 6: Variation of RCS of two layer coated PEC circular cylinder of radius *a*=60 mm; thickness of coatings is $t_1=t_2$=30 mm. DPS-DNG coating, $\varepsilon_{r1=}$4, $\mu_{r1=}$2, $\varepsilon_{r2=}$-4, $\mu_{r2=}$-2; *f*=5 GHz; TM$_z$ polarization

Further, the variation of RCS of two layer coated PEC cylinder with frequency is analyzed. Here PEC cylinder radius is 50 mm (*a*=50 mm) with two layers of DNG coatings. The constitutive parameters of the coatings are t_1=2 mm, t_2=1 mm, $\varepsilon_{r1=}$-4, μ_{r1}=-2, $\varepsilon_{r2=}$4, $\mu_{r2=}$2. The variation of cylinder RCS with frequency (1-19 GHz) for TM$_z$ polarization is shown in Figure 7. It is apparent that the RCS reduction has been achieved only over a particular range of frequencies (7-8.6 GHz).
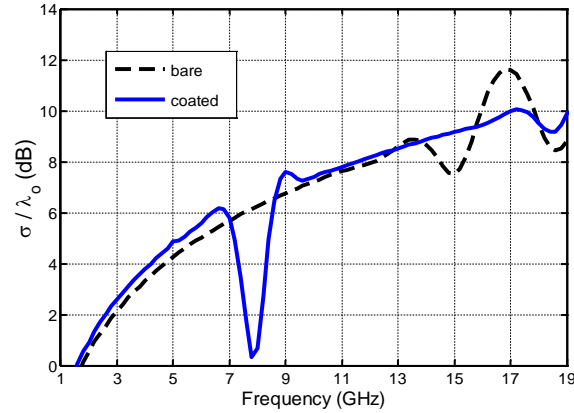
Figure 7: Comparison of RCS of a conducting bare and two layer metamaterial-coated PEC infinitely long circular cylinder; t_1=2 mm, t_2 =1 mm, $\varepsilon_{r1=}$-4, $\mu_{r1=}$-2, $\varepsilon_{r2=}$4, $\mu_{r2=}$2; TM$_z$ polarization

As a next case, the same PEC cylinder (*a*=50 mm) is considered, with two layer coating of DNG material. The first coating is 2 mm thick (*b*=52 mm), second coating is of 1 mm thickness (*c*=53 mm). The material parameters are $\varepsilon_{r1=}$-5, $\mu_{r1=}$-2, $\varepsilon_{r2=}$-6, $\mu_{r2=}$-3. The variation of cylinder RCS with frequency has been computed for TE$_z$ polarization (Figure 7). It may be observed that the cylinder RCS is reduced over the frequency range of 11.2-12.8 GHz.
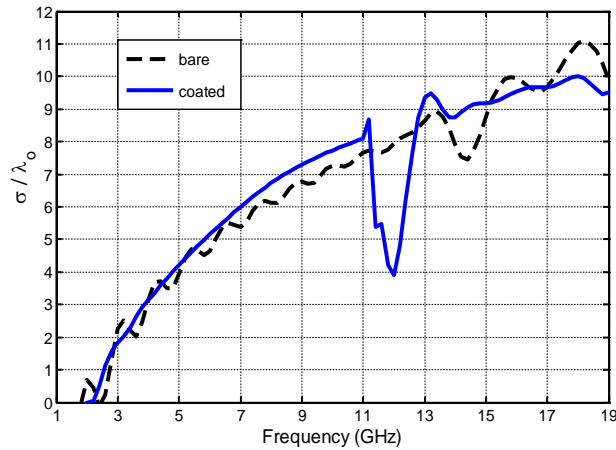

Figure 8: Comparison of RCS of a conducting bare and two layer metamaterial-coated PEC infinitely long circular cylinder; t_1=2 mm, t_2 =1 mm, $\varepsilon_{r1=}$-5, $\mu_{r1=}$-2, $\varepsilon_{r2=}$-6, $\mu_{r2=}$-3; TE$_z$ polarization

In order to get clearer understanding of the RCS behavior of single layer metamaterial coated PEC cylinder, the contour plots for RCS of circular PEC cylinder for different thickness *t*, of metamaterial coating are shown for TE$_z$ polarization (Figure 8) and TM$_z$ mode (Figure 9). The radius of PEC cylinder is taken as *a*=50 mm at *f*=5 GHz. The permittivity and permeability of the metamaterial coating are varied from 0 to -30. The

contour plots for different thicknesses of coating are compared using a common scale. The color of contour shows the level of cylinder RCS. The darker blue (indigo) colored regions of the plots represent the combination of ε_{r1} and μ_{r1} which yield lowest RCS, while red corresponds to the combination which gives highest RCS. Further it may be observed that for thin coating the cylinder RCS is low for most of the combinations of ε_{r1} and μ_{r1}. As the thickness of coating increases, the RCS value increases.

Next, the RCS of two layer metamaterial coated PEC circular cylinder (a=50 mm) is computed as a function of both frequency and thickness (t_1) of Layer 1. The contour plots for different values of thickness (t_2) of Layer 2, for the TM$_z$ polarization is shown in Figure 10. The material parameters of coatings are same as those in Figure 7. The contour plots are compared with that of a bare cylinder. It is apparent that, the cylinder RCS is reduced in certain frequency ranges (represented by the dark blue color). Moreover increase in RCS is observed at higher frequencies (red color). As thickness of Layer 2 is increased, higher RCS reduction is achieved, but limited to low frequency range. A similar trend has been observed in TE$_z$ polarization (Figure 11) for doubly coated cylinder with constitutive parameters of Figure 8.
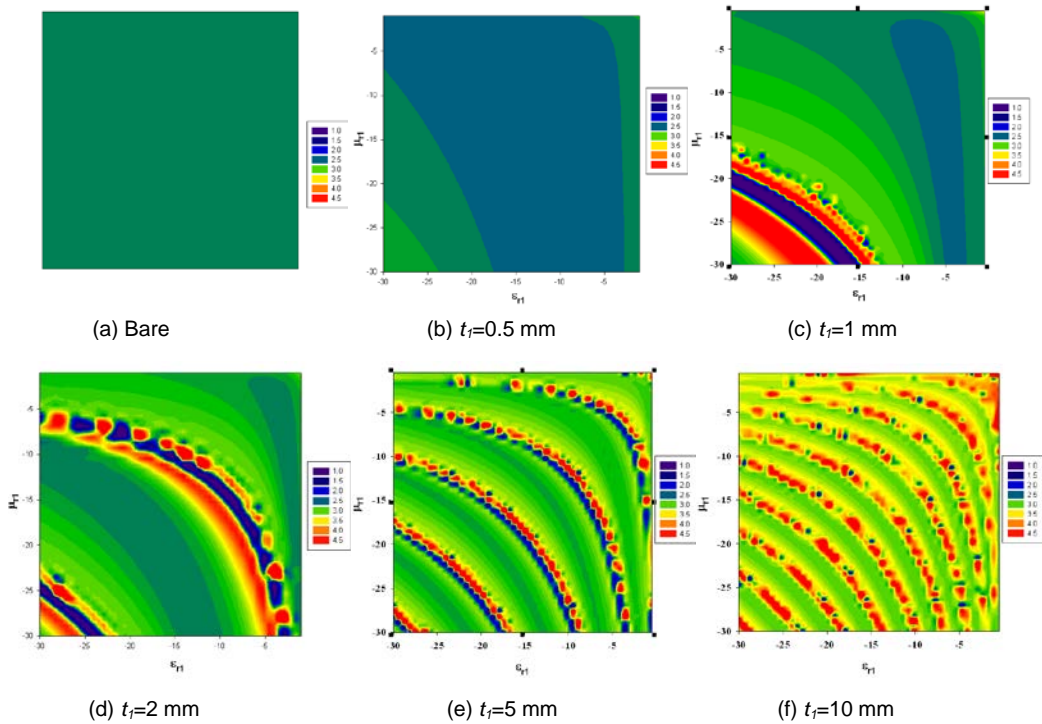

(a) Bare   (b) t_1=0.5 mm   (c) t_1=1 mm

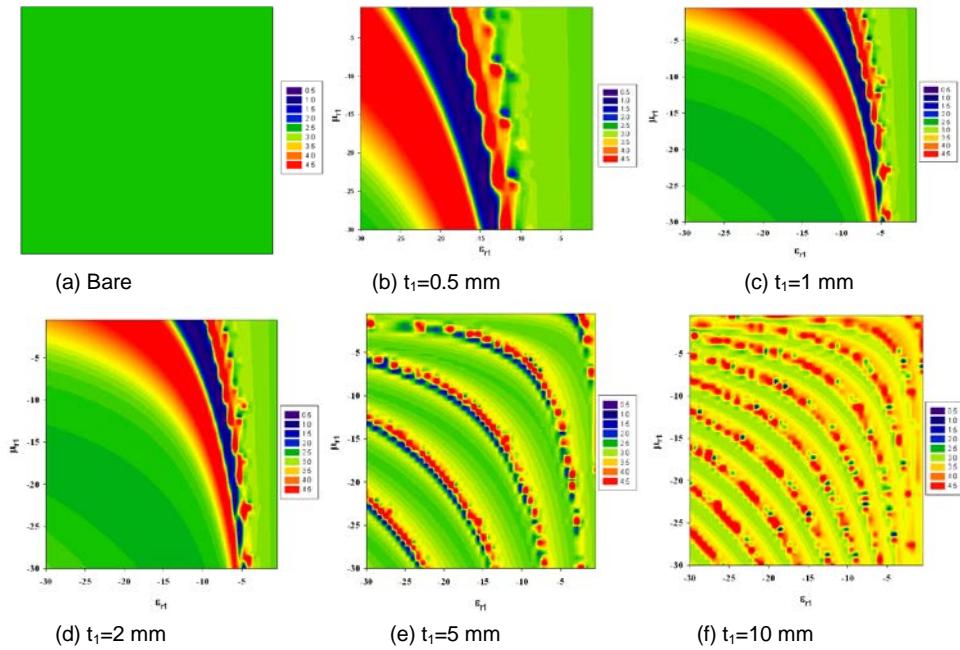(d) t_1=2 mm   (e) t_1=5 mm   (f) t_1=10 mm

Figure 9: Contour plots showing RCS variation of a single layer metamaterial coated PEC cylinder (a=50 mm) with permittivity and permeability, for different values of thickness t_1; TE$_z$ polarization

(a) Bare   (b) t₁=0.5 mm   (c) t₁=1 mm

(d) t₁=2 mm   (e) t₁=5 mm   (f) t₁=10 mm
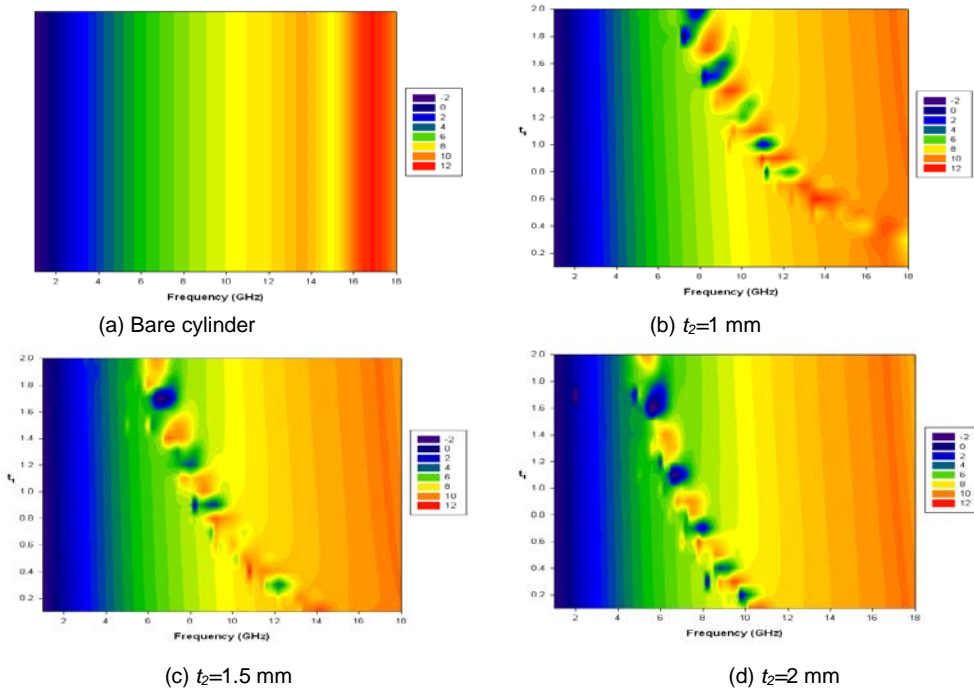
Figure 10: Contour plots showing RCS variation of a single layer metamaterial coated PEC cylinder (*a*=50 mm) with permittivity and permeability, for different values of thickness t_1; TM$_z$ polarization

(a) Bare cylinder   (b) t_2=1 mm

(c) t_2=1.5 mm   (d) t_2=2 mm
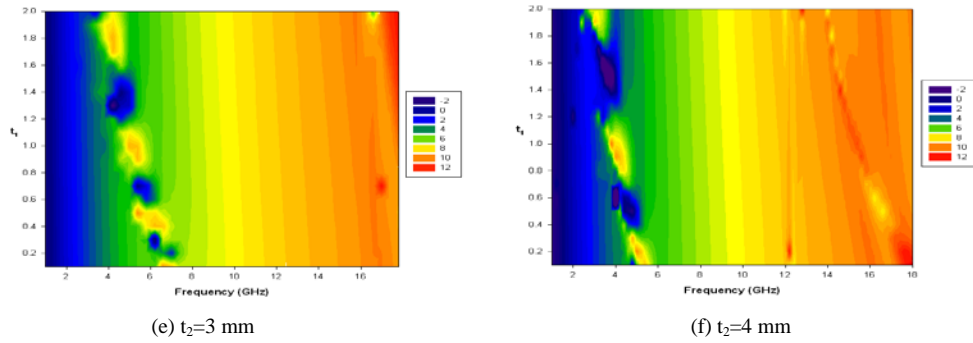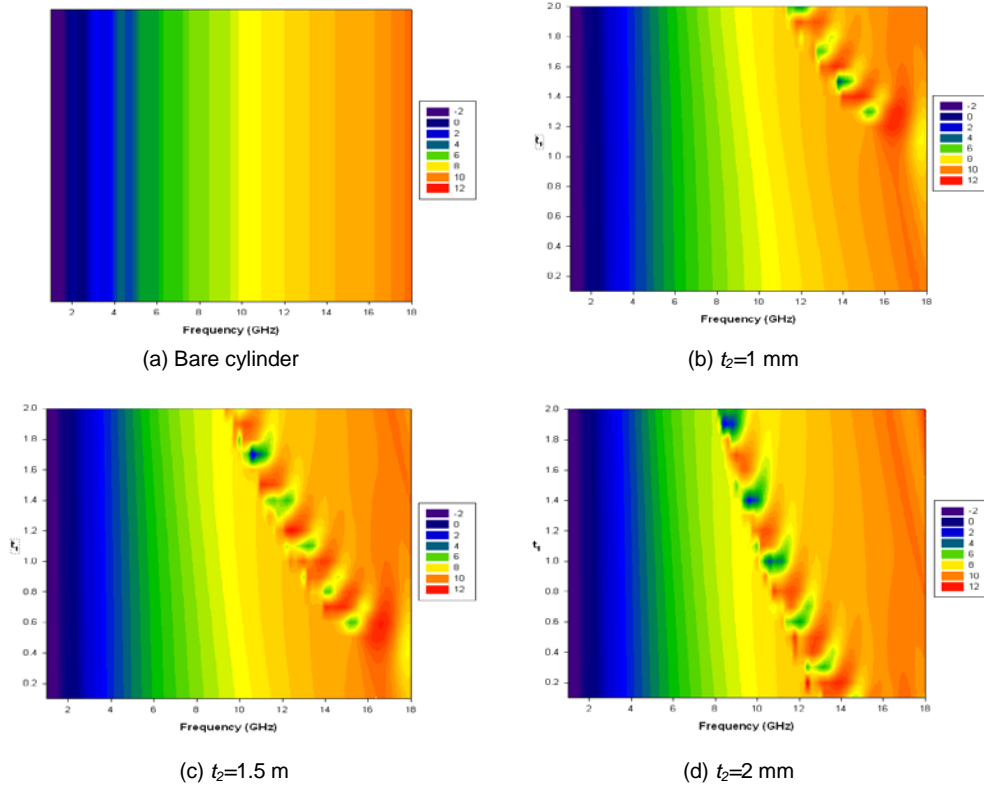
(e) t₂=3 mm

(f) t₂=4 mm

Figure 11: Contour plots showing RCS variation of a two layer metamaterial coated PEC cylinder (a=50 mm) with thickness t_1 of Layer 1 and frequency f; ε_{r1}=-2.5, μ_{r1}=-1, ε_{r2}=-9.8 and μ_{r2}=-3; TM$_z$ polarization

(a) Bare cylinder

(b) t_2=1 mm

(c) t_2=1.5 m

(d) t_2=2 mm

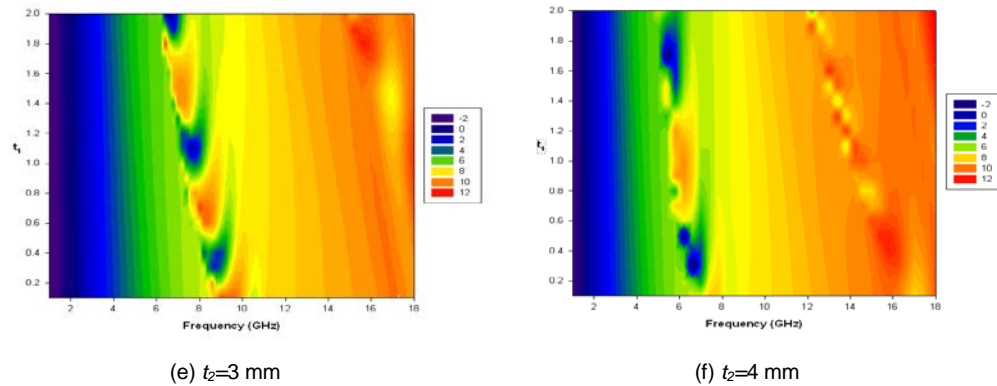(e) t_2=3 mm   (f) t_2=4 mm

Figure 12: Contour plots showing RCS variation of a two layer metamaterial coated PEC cylinder (a=50 mm) with thickness t_1 of Layer 1 and frequency f; ε_{r1}=-5, μ_{r1} = 2, ε_{r2} =-6 and μ_{r2} =3; TE$_z$ polarization

4 Conclusions

Metamaterial due to its peculiar EM characteristics attracts the attention of researchers towards RCS control. In this paper, a PEC infinitely long circular cylinder with metamaterial coating is studied based on analytical approach. The incident and scattered field components are analytically derived in terms of Bessel and Hankel functions, imposing appropriate boundary conditions. It is shown that TM$_z$ polarization contributes more to the RCS of the structure as compared to TE$_z$ polarization. However RCS reduction is obtained only at certain frequencies in TM$_z$ polarization. This may be due to constitutive parameters considered for coating material. This further emphasizes the need of optimization of material characteristics of coating.

For TM$_z$ polarization, cylinder RCS is higher for large permittivity and small permeability of the coating. On the other hand, for TE$_z$ polarization, cylinder RCS is high when permittivity of coating is low and permeability is large. For single layer metamaterial coating, the RCS increases with thickness. For a PEC circular cylinder coated with two layers either metamaterial or dielectric coating RCS reduction can be achieved but for certain frequency ranges. In case of two-layer coating, with both layers chosen as DNG, as the thickness of the metamaterial coating increases, the cylinder RCS decreases significantly over certain low frequency ranges. This feature can be further improved by more rigorous optimization of coating parameters.

References

Balanis, C. A. (2012): *Advanced Engineering Electromagnetics* (ed. 2). John Wiley & Sons, USA, ISBN 978-0-470-58948-9, pp.1040

Capolino, F. (2009): *Theory and Phenomena of Metamaterials*. CRC Press, USA, ISBN: 978-1-4200-5425-5, pp. 926.

Chaurasiya, D.; Ghosh, S.; Srivastava, K. V. (2014): Dual band polarization-insensitive wide angle metamaterial absorber for radar application. *Proceedings of European Microwave Conference,* pp. 885-888.

Crispin, J. W.; Siegel, K. M. (1968): *Methods of Radar Cross Section Analysis.* Academic Press, USA, ISBN: 978-0-1219-7750-4, pp. 426.

Eugene, F. K. (1985): A progression of high-frequency RCS prediction techniques. *Proceedings of IEEE*, vol. 73, no. 2, pp. 252-264.

Irci, E.; Erturk, V. B. (2007): Achieving transparency and maximizing scattering with metamaterial-coated conducting cylinders. *Physical Review E*, no. 76, pp. 056603-(1-15).

Jenn, D. C. (2005): *Radar and Laser Cross Section Engineering*. AIAA Press, USA, ISBN: 978-1563477027, pp. 505.

Kwon, S. H.; Lee, H. K. (2009): A Computational Approach to Investigate Electromagnetic Shielding Effectiveness of Steel Fiber-Reinforced Mortar. *Computers, Materials & Continua*, vol. 12, no. 3, pp. 197.

Li, C.; Shen, Z. (2003): Electromagnetic scattering by a conducting cylinder coated with metamaterials. *Progress in Electromagnetics Research*, vol. 42, pp. 91-105.

Sakr, A. A.; Soliman, E. A.; Abdelmageed, A. K. (2014): An integral equation formulation for TM scattering by a conducting cylinder coated with an inhomogeneous dielectric/magnetic material. *Progress in Electromagnetics Research B*, vol. 60, pp. 49-62.

Shi, J.; Liu, R.; Wang, Z.; Fu, T. (2010): Positive and negative metamaterials as frequency selective surface. *SPIE Proceedings*, vol. 7854, pp. 78543O (1-5).

Smith, D. R.; Padilla, W. J.; Vier, D. C.; Schultz, S.; Nasser, S. C. N. (2000): Composite medium with simultaneously negative permeability and permittivity. *Physical Review Letters*, vol. 84, no. 18, pp. 4184-4187.

Soares Jr, D. (2009)**:** Numerical modelling of electromagnetic wave propagation by meshless local Petrov-Galerkin formulations. *Computer Modeling in Engineering and Sciences*, vol. 19, no. 2, pp. 97.

Wu, X.; Hu, C.; Wang, M.; Pu, M.; Luo, X. (2015): Realization of low scattering metamaterial shell based on cylindrical wave expanding theory. *Optics Express*, vol. 23, no. 8, pp. 10396-10404.

Yao, H. Y.; Li, L. W.; Qiu, C. W. (2006): Electromagnetic scattering properties in a multilayered metamaterial cylinder. *IEEE Mediterranean Electro Technical Conference*, pp. 246-249.

Zainud-Deen, S. H.; Botros, A. Z.; Ibrahim, M. S. (2008): Scattering from bodies coated with metamaterial using FDFD method. *Progress in Electromagnetics Research B*, vol. 2, pp. 279-290.

Ziolkowski, R. W.; Heyman, E. (2001): Wave propagation in media having negative permittivity and permeability. *Physical Review. E*, vol. 64, no. 5, pp. 056625 (1-15).